

Exploring Anti-Aging Potential of *Dendrobium* Species and Novel Microemulsion Delivery of *Dendrobium kentrophyllum* Extract for Anti-Aging Effect

Suradwadee Thungmungmee¹, Boonchoo Sritularak², Nakuntwalai Wisidsri¹, Nattakan Kanana³, Nattika Nimmano³

¹Faculty of Integrative Medicine, Rajamangala University of Technology Thanyaburi, Pathum Thani, Thailand; ²Department of Pharmacognosy and Pharmaceutical Botany, Faculty of Pharmaceutical Science, Chulalongkorn University, Bangkok, Thailand; ³Department of Pharmaceutics and Industrial Pharmacy, Faculty of Pharmaceutical Sciences, Chulalongkorn University, Bangkok, Thailand

Correspondence: Nattika Nimmano, Department of Pharmaceutics and Industrial Pharmacy, Faculty of Pharmaceutical Sciences, Chulalongkorn University, Bangkok, Thailand, Tel +66 0 2188399, Fax +66 0 2188401, Email nattika.n@pharm.chula.ac.th

Purpose: The study aimed to investigate in vitro anti-aging activities of 29 *Dendrobium* spp. and develop and characterize microemulsions (MEs) for topical application.

Methods: Antioxidant activity was determined using 2,2-diphenyl-1-picrylhydrazyl (DPPH), H₂O₂ scavenging, and ferric reducing antioxidant power (FRAP) assays. The anti-collagenase (MMP-1 and MMP-2) and anti-elastase activities were also evaluated. Cytotoxicity and human intracellular reactive oxygen species (ROS) levels were determined using resazurin reduction and 2',7'-dichlorofluorescein diacetate (DCFDA) assays, respectively. *D. kentrophyllum* extract-loaded microemulsion (DKME) was then prepared and optimized. The stability of DKME was studied using a heating-cooling cycle.

Results: *D. kentrophyllum* appeared to be the best candidate anti-aging agent because of its antioxidant, anti-collagenase, and anti-elastase activities. The extract was safe for human skin cells at a concentration of 6.25–100 µg/mL. It also decreased the intracellular ROS-induced ultraviolet B (UVB) irradiation compared to that in the control. DKME comprising Tween 80:ethanol (5:1), water, and isononyl isononanoate showed a suitable appearance, droplet size, polydisperse index, zeta potential, pH, and viscosity. This formulation demonstrated desirable physical and chemical stability, with non-cytotoxic effects.

Conclusion: DKME is considered a promising anti-aging product. However, an in vivo study of this optimized formulation might be evaluated in further study for anti-aging purposes.

Keywords: reactive oxygen species, anti-aging activities, *Dendrobium kentrophyllum*, microemulsion

Introduction

The skin is the main visible sign of aging. It is characterized by wrinkles, loss of elasticity, laxity, and rough-textured appearance. The majority (80%) of facial aging is affected by extrinsic factors, particularly ultraviolet (UV) radiation exposure, whereas only 3% is caused by intrinsic factors. UV radiation induces the production of reactive oxygen species (ROS), which considerably accelerates the aging process. ROS are free radicals or oxidants, including superoxide anion radical (O₂^{•-}), hydroxyl radicals (•OH), hydrogen peroxide (H₂O₂), singlet oxygen (¹O₂), nitric oxide (NO), and peroxynitrite (ONOO⁻).¹ In intracellular dermal cells, ROS induce matrix metalloproteinases (MMPs) expression in dermal fibroblasts and epidermal keratinocytes. MMPs stimulate degradation of the components of the extracellular matrix (ECM) and epidermal-dermal adhesion.² ECM is mainly composed of fibrous proteins, such as collagen and elastin. Collagen is stable and resistant to proteolytic cleavage. However, an increase in MMPs, particularly interstitial collagenase (MMP-1), in the ECM promotes collagen type I and III fragmentation. MMP-2 or gelatinase can cleave collagen type IV in the epidermal basement membrane and collagen type I. Moreover, elastin degradation by elastase accelerates skin aging.³

Antioxidants are effectively used in skincare products and supplements to reduce ROS production. Several studies have reported that several plant families revealed the potential anti-aging properties through antioxidant, anti-collagenase, and anti-elastase activities, ie, Annonaceae, Primulaceae, Fabaceae, Zingiberaceae, Phyllanthaceae, Theaceae, and Orchidaceae.^{4–8}

Dendrobium, also called Shihu or Huangcao, is one of the largest genera in the Orchidaceae family. More than 1,500 species have been identified worldwide.⁹ The stems of *Dendrobium* species have been used in traditional Chinese medicine. *Dendrobium* species have demonstrated biological activities and efficacy in medicinal uses, such as hepatic lipid and gluconeogenesis regulation, neuroprotection, anti-tumor, anti-inflammatory, anti-diabetes, anti-virus factors, and dermatological disorders.^{8,10,11} The chemical constituents of *Dendrobiums* are alkaloids, coumarins, bibenzyls, fluoronones, phenanthrenes, and sesquiterpenoids.¹²

Polysaccharides from *D. officinale*, *D. candidum*, and *D. cv. Khao Sanan* displayed antioxidant capability, skin moisturizing effects, and inhibition of the MMP-2 expression.^{13–15} The fermented extract of *D. officinale* showed high radical scavenging activities. *Dendrobium* Sonia Earsakul flowers inhibit collagenase and elastase activities and MMP-2 in fibroblast cells.¹⁶ (–)-Dendroparishiol, a bibenzyl compound in *D. parishii*, showed the highest antioxidant activities (peroxyl radical; ROO-, DPPH radical, and hydroxyl radical; (OH)).¹⁷ It significantly decreased ROS in H₂O₂-treated RAW264.7 cells, decreased nitric oxide and TNF- α secretion, and enhanced antioxidant enzyme (superoxide dismutase; SOD, catalase; CAT, glutathione peroxidase; GPx) activities in a dose-dependent manner. The antioxidant activity of phenolic compounds in *D. loddigesii* such as crepidatin, moscatilin, 4,5,4'-trihydroxy-3,3'-dimethoxybibenzyl, 4',5-dihydroxy-3,3'-dimethoxybibenzyl, and *p*-dihydroconiferyl dihydro-*p*-coumarate showed a high percentage of DPPH radical scavenging in the range of 89.411 to 93.391.¹⁸ Although *Dendrobium* has been found in approximately 150 species in Thailand, studies on their properties against the skin aging process are still limited.

It is challenging to utilize natural extracts in topical formulations, such as creams, lotions, and gels, because they have low solubility and skin permeation. Microemulsions (MEs) are isotropic, thermodynamically stable mixtures with an appropriate proportion of oil, water, and surfactants with droplet sizes in the range of 10–200 nm.¹⁹ MEs have been used in dermal delivery systems owing to their ease of preparation and scale-up, increased solubilization of therapeutic agents, enhanced skin permeability, increased thermodynamic stability, and reduced possibility of toxicity.²⁰ It has been reported that natural extracts are incorporated into microemulsion systems. For instance, the potential antioxidant and anti-collagenase properties of citrus essential oils from *Citrus aurantifolia* and *Citrus reticulata* loaded in microemulsions could reduce skin irritation in human volunteers and apply for anti-aging.²¹ *Cordyceps militaris* extract, which exhibited MMP-1 and elastase activities, was incorporated into microemulsions. This formulation significantly improved skin moisture and elasticity without side effects. As a result, it was recommended as an effective formulation for anti-wrinkles.²²

Therefore, this study aimed to investigate the biological anti-aging activities of 29 *Dendrobium* plant extracts using antioxidant, anti-collagenase, and anti-elastase assays. The most effective *Dendrobium* was evaluated for its cytotoxicity and prevention of intracellular ROS. *Dendrobium* extract-loaded MEs were developed for characterization, stability, and cytotoxicity studies.

Materials and Methods

Chemicals and Reagents

Clostridium histolyticum collagenase (EC 3.4.24.3, CAS No. 9001–12-1), N-[3-(2-Furyl)acryloyl]-L-leucyl-glycyl-L-prolyl-L-alanine (FALGPA) (CAS No. 78832–65-2), 2',7'-Dichlorofluorescein diacetate (DCFDA), and resazurin was purchased from Sigma-Aldrich (USA). Standard epigallocatechin gallate (EGCG; CAS No. 989–51-5), gallic acid (CAS No. 149–91-7), quercetin (CAS No. 6151–25-3), and L-ascorbic acid (CAS No. 50–81-7) were purchased from Sigma-Aldrich (USA). Ferrous sulfate heptahydrate (FeSO₄·7H₂O) (CAS No. 7782–63-0) and TPTZ were purchased from LOBA CHEMIE, India. The EnzChek[®] Gelatinase/Collagenase Assay Kit (Lot No. 2281586, Invitrogen[™], Thermo Fisher Scientific, Oregon, USA), EnzChek[®] Elastase Assay Kit (Lot No. 2397740, Invitrogen[™], Thermo Fisher Scientific, Oregon, USA), and 96-well microplates for fluorescence-based assays were purchased from Molecular

Probes (Eugene, Oregon, USA). Analytical grade ethyl alcohol (CAS No. 64–17-5), hydrogen peroxide (CAS No. 7722–84-1), and high-performance liquid chromatography (HPLC) were purchased from RCI Labscan, Thailand. Sodium acetate was purchased from Fisher Scientific (UK). Ferric chloride hexahydrate ($\text{FeCl}_3 \cdot 6\text{H}_2\text{O}$; CAS No. 10025–77-1) was purchased from QReC™ (New Zealand). Dulbecco's modified Eagle's medium (DMEM), trypsin-EDTA, fetal bovine serum (FBS), and penicillin were purchased from Gibco (Carlsbad, CA, USA). Tween 80 (CAS No. 9005–65-6) and isononyl isononanoate (CAS No. 42131–25-9) were purchased from CHEME COSMETICS (Thailand).

Plant Materials

The 29 *Dendrobium* methanolic extracts were obtained from Assoc. Prof. Dr. Boonchoo Sritularak, Department of Pharmacognosy and Pharmaceutical Botany, Faculty of Pharmaceutical Science, Chulalongkorn University, Thailand.

Antioxidant Properties of *Dendrobium* Extracts

2,2-Diphenyl-1-Picrylhydrazyl (DPPH) Free Radical Scavenging Activity

Briefly, 20 μL of the extract at 100 $\mu\text{g/mL}$ was mixed with 180 μL of 0.02 mM DPPH solution. After incubation for 30 minutes at room temperature in the dark, the absorbance of the mixture was measured at 517 nm against a blank solution. *L*-ascorbic acid was used as a positive control.²³ The concentration of the sample required to scavenge 50% DPPH radicals (IC_{50}) was calculated.

Hydrogen Peroxide (H_2O_2) Scavenging Assay

Briefly, 80 μL of the extract (100 $\mu\text{g/mL}$) was added to 720 μL H_2O_2 solution (40 mM) in phosphate buffer (pH 7.4). After 10 minutes, the absorbance of the mixture was measured at 230 nm against a blank solution. *L*-ascorbic acid was used as a positive control.²⁴ The concentration of the sample required to scavenge H_2O_2 by 50% (IC_{50}) was calculated.

Ferric Reducing Antioxidant Power (FRAP)

The FRAP reagent was prepared by mixing 100 mL of 300 mM sodium acetate (adjusted to pH 3.6 by glacial acetic acid), 10 mL of 20 mM $\text{FeCl}_3 \cdot 6\text{H}_2\text{O}$, and 10 mL of 10 mM TPTZ solution (dissolved in 40 mM HCl). The assay was performed by mixing 20 μL of the extract (100 $\mu\text{g/mL}$) and 180 μL of FRAP reagent. The mixture was then incubated at 37°C for 30 minutes. Absorbance was measured at 593 nm. $\text{FeSO}_4 \cdot 7\text{H}_2\text{O}$ and distilled water were used as the standard and blank, respectively.^{25,26} The FRAP values were presented as mmol FE/g dry extract with the calibration curve of Fe^{2+} .

Enzyme Inhibition

MMP-1 Inhibitory Activity

MMP-1 inhibitory activity was determined based on a spectrophotometric method, with slight modifications.²⁷ Briefly, *Clostridium histolyticum* collagenase was dissolved in ultrapure water at a concentration of 4 units/mL. The synthetic substrate FALGPA was dissolved in 50 mM Tricine buffer (pH 7.5 with 400 mM NaCl and 10 mM CaCl_2) to 1 mM. Four microliters of extract (100 $\mu\text{g/mL}$) was mixed and equilibrated at 25°C with 145 μL substrate before adding 4 μL of enzyme to start the reaction. The control sample was prepared in water. The absorbance at 335 nm was measured immediately after addition of the enzyme and left for 20 minutes. EGCG was used as a positive control. The percentage of MMP-1 inhibition was calculated.

MMP-2 Inhibitory Activity

The MMP-2 inhibitory activity was determined using the EnzChek® Gelatinase/Collagenase Assay Kit. This was modified by Pientaweeratch et al.⁶ Then, 80 μL extract (100 $\mu\text{g/mL}$), 20 μL of 2.5 $\mu\text{g/mL}$ DQ gelatin, and 100 μL 0.0375 U/mL collagenase were mixed in a black 96-well plate. The mixture was then incubated for 10 minutes at room temperature under light-protected conditions. The fluorescence intensity was measured at the excitation and emission wavelengths of 480 and 530 nm, respectively. 1.10-phenanthroline and EGCG were used as the inhibitors and positive controls, respectively. The percentage of MMP-2 inhibition was calculated.

Elastase Inhibitory Activity

Elastase inhibitory activity was determined using the EnzChek[®] Elastase Assay Kit, with some modifications (Pientaweeratch et al, 2016).⁶ TM elastin was used as a substrate. In the test, 50 µL extracts (100 µg/mL), 50 µL of 25 µg/mL DQTM elastin, and 100 µL 0.2 U/mL elastase were mixed in a black 96-well plate. The mixture was then incubated for 5 minutes at room temperature under light-protected conditions. The fluorescence intensity was measured at the excitation and emission wavelengths of 480 and 530 nm, respectively. *N*-Methoxysuccinyl-Ala-Ala-Pro-Val-chloromethyl ketone and EGCG were used as the inhibitor and positive control, respectively. The percentage of elastase inhibition was calculated.

Isolation of *Dendrobium kentrophyllum*

D. kentrophyllum (Supplementary Figure S1) was dried and extracted using the maceration technique. Crude methanolic extract of *D. kentrophyllum* was partitioned with ethyl acetate, butanol, and water to yield the ethyl acetate, butanol, and aqueous extracts. The partition extracts were separated and fractionated by vacuum-liquid chromatography and column chromatography (Supplementary Figure S2).

Cytotoxic Evaluation

The cytotoxicity of *D. kentrophyllum* extract was assessed using a resazurin reduction assay with some modifications by Zhu et al.²⁸ Human fibroblast (BJ) (Lot No. 70015964, ATCC[®]-CRL-2522, USA) and human keratinocytes (HaCaT) (Lot No. 300493–524, Cell Lines Service, Eppelheim, Germany) were seeded in a 96-well plate at a concentration of 2×10^5 cells/mL and incubated at 37°C in a humidified atmosphere of 5% CO₂ for 24 hours. The samples were diluted in a culture medium to a final concentration of 100–6.25 µg/mL, and then BJ or HaCaT cells were treated with the samples for 24 hours. The treated cells were incubated with 50 µg/mL resazurin at 37°C and 5% CO₂ for 4 hours. Absorbance was measured at 560 and 600 nm. Cell viability was determined by comparing the percentage of viable cells with that of the solvent control.

To evaluate the cytotoxicity of *D. kentrophyllum* extract-loaded microemulsions (DKME) and microemulsion base (MEB), the samples were diluted in culture medium into the final concentration of 200–6.25 µg/mL using the above-mentioned assay.

Inhibition of Intracellular ROS

Intracellular ROS levels were determined using the DCFDA assay with minor modifications (Xiao et al, 2020).²⁹ Non-cytotoxic concentrations of *D. kentrophyllum* extract and its major compounds were added to BJ or HaCaT cells for 24 hours. Treated cells were washed twice with PBS (pH 7.4) and irradiated with UVB (40 mJ/cm²). DCFDA (50 µM) was then added and incubated at 37°C and 5% CO₂ for 30 minutes. The treated cells were washed twice with PBS. ROS quantity was determined by measuring the fluorescence intensity at 485 nm excitation and 535 nm emission using a fluorescence microplate reader. The percentage of ROS generated was calculated and compared with that of the control.

Development of MEs

Construction of Phase Diagram

Pseudo-ternary phase diagrams were constructed by mixing different concentrations of oil, a mixture of surfactants and cosurfactants (Smix), and DI water (w/w) to determine the optimal composition of the MEs region. Smix was prepared by combining a surfactant (Tween 80) and cosurfactant (ethanol) at ratios of 1:1, 3:1, and 5:1. The oil phase, isononyl isononanoate, was then mixed, and water was subsequently titrated. The ME formulations were examined using a cross-polarizer and plotted as phase diagrams. The area of the MEs region was determined using CHEMIX school software. The MEs in which the resulting mixtures formed transparently were subsequently selected from the phase diagram.

Preparation of *D. Kentrophyllum* Extract-Loaded ME Formulation

As stated in the result of IC₅₀ by DPPH and H₂O₂ assays, 0.4%w/w of *D. kentrophyllum* extract (more than 10 times of IC₅₀) was used. The extract was completely dissolved in a mixture of Smix and oil using a magnetic stirrer at 400 rpm for 12 hours. DI water was then gradually added and continuously mixed for 15 minutes.

Characterization of ME Formulations

The optical properties of DKME and MEB were characterized by small-angle X-ray scattering (SAXS) analysis, droplet size, polydispersity index (PDI), zeta potential, pH, and viscosity. Optical properties were examined using cross-polarized light microscopy (Olympus U-HSEXP, Tokyo, Japan). The structural evaluation of the formulations was performed using SAXS (Anton Paar SAXSPoint 2.0, Austria). 2D data and scattered intensities were detected using a linear position-sensitive detector. The average size, PDI, and zeta potential of the formulations were measured using a Nanoparticle Analyzer (NanoParticle SZ-100V2 Series, HORIBA, Japan) at 25°C with a scattering angle of 175°. The pH was directly measured using a pH meter at 25°C. Viscosity was measured using an LVDV-II+ Brookfield viscometer (Brookfield Engineering Laboratories, Inc., Middleborough, Massachusetts, US) with spindle number LV-3 and a speed of 90 rpm. All data were reported in triplicate.

Stability Test of ME Formulations

The physical and chemical stabilities of DKME and MEB were investigated over eight heating-cooling cycles. In each cycle, the samples were maintained at 45°C for 24 hours and 4°C for 24 hours. Physical stability was evaluated in terms of appearance, droplet size, PDI, zeta potential, pH, optical properties, and viscosity, as described above. The degradation of quercetin, an active compound in *D. kentrophyllum* extract, was determined using the validated high-performance liquid chromatography (HPLC) method described by Thiangtham et al.³⁰

Statistical Analysis

All experiments were performed in triplicate and are reported as mean \pm standard deviation. Statistical analysis was carried out by one-way ANOVA followed by Tukey's post-hoc test or paired *t*-test using SPSS 24.0. Statistical significance was set at $p < 0.05$.

Results

Antioxidant Activities

The antioxidant activities of *Dendrobium* extracts are presented in Table 1. For the DPPH assay, *D. kentrophyllum* showed antioxidant capacity with IC_{50} of 26.58 ± 6.87 $\mu\text{g/mL}$, which is significantly different from that of the other *Dendrobium*, except for *D. brymerianum* (IC_{50} of 30.04 ± 2.81 $\mu\text{g/mL}$). However, this activity was lower than *L*-ascorbic acid, which had an IC_{50} of 7.43 ± 0.31 $\mu\text{g/mL}$. *D. brymerianum* showed the highest H_2O_2 scavenging capacity, with an IC_{50} of 53.7 ± 1.71 $\mu\text{g/mL}$. The IC_{50} of *L*-ascorbic acid was 156.33 ± 1.68 $\mu\text{g/mL}$, which was lower than that of the extract. The ferric ion-reducing antioxidant power of the extracts was related to DPPH and H_2O_2 scavenging activities. The values ranged from 1.31 to 22.31 mmol FE/mg dry extract. *D. kentrophyllum* showed the strongest ferric ion reducing power, being 22.31 ± 0.34 mmol FE/mg dry extract.

Anti-Collagenase and Anti-Elastase Activities

All *Dendrobium* extracts inhibited MMP-1 and MMP-2 activities, whereas some extracts inhibited elastase activity (Table 1). The MMP-1 inhibitory activity of the 29 *Dendrobium* extracts ranged from 34.13% to 49.87%. *D. brymerianum* showed the highest MMP-1 inhibitory effect ($49.87 \pm 1.80\%$). EGCG had a significantly higher value than the other extracts ($p < 0.05$).

The MMP-2 inhibitory activity of the extracts varied from 14.02% to 94.96%. *D. kentrophyllum* showed the highest MMP-2 inhibitory effect, at $94.96 \pm 1.40\%$, which was not significantly different ($p > 0.05$) from that of EGCG.

The elastase inhibitory activity ranges from 5.21% to 36.45%. *D. venustum* showed the highest activity ($36.45 \pm 3.60\%$); however, these anti-elastase activities were lower than those of EGCG.

Phytochemical Investigation of *D. Kentrophyllum*

The methanol extract prepared from dried whole plants of *D. kentrophyllum* showed the highest total phenolic content (TPC) and total flavonoid content (TFC) (Supplementary Table S1). It also exhibits antioxidant and anticollagenase

Table 1 Antioxidant Activities (n=3), Anti-Collagenase (MMP-1 and MMP-2), and Anti-Elastase Activities of 29 Dendrobium Extracts (n=2)

No.	Scientific Name	H ₂ O ₂ Scavenging Activity (IC ₅₀ , µg/mL)	DPPH Scavenging Activity (IC ₅₀ , µg/mL)	FRAP value, mmol FE/ mg Dry Extract	%MMP-1 Inhibition (at 100 µg/mL)	%MMP-2 Inhibition (at 100 µg/mL)	%Elastase Inhibition (at 100 µg/mL)
1	<i>D. signatum</i>	> 100	> 100	5.09 ± 0.35	44.73 ± 2.57	64.02 ± 0.81	12.43 ± 3.44
2	<i>D. tortile</i>	> 100	> 100	4.80 ± 0.42	41.02 ± 1.74	57.34 ± 5.94	12.92 ± 0.87
3	<i>D. brymerianum</i>	53.7 ± 1.71	30.04 ± 2.81	23.88 ± 1.22	49.87 ± 1.80	33.29 ± 1.80	ND
4	<i>D. findlayanum</i>	> 100	> 100	2.97 ± 0.26	44.00 ± 1.60	46.09 ± 0.97	ND
5	<i>D. delacourii</i>	> 100	66.14 ± 3.40	9.23 ± 0.85	39.27 ± 3.12	55.59 ± 1.61	8.98 ± 3.03
6	<i>D. scabrilingue</i>	> 100	> 100	5.95 ± 0.56	43.62 ± 2.11	58.99 ± 4.85	32.18 ± 0.52
7	<i>D. albosanguineum</i>	> 100	> 100	6.42 ± 0.41	44.54 ± 4.87	86.71 ± 6.13	32.25 ± 7.30
8	<i>D. formosum</i>	73.33 ± 2.03	75.05 ± 11.56	10.21 ± 0.87	40.87 ± 1.15	87.94 ± 7.95	35.74 ± 2.71
9	<i>D. virgineum</i>	> 100	> 100	4.50 ± 0.28	36.73 ± 0.65	51.78 ± 7.67	ND
10	<i>D. moschatum</i>	> 100	> 100	3.53 ± 0.48	38.36 ± 3.90	46.52 ± 9.63	10.27 ± 0.68
11	<i>D. infundibulum</i>	69.18 ± 0.16	58.29 ± 1.80	7.94 ± 0.63	35.07 ± 2.79	74.08 ± 7.11	32.64 ± 2.21
12	<i>D. venustum</i>	69.47 ± 0.01	81.94 ± 7.95	10.33 ± 0.76	36.51 ± 2.98	63.51 ± 0.31	36.45 ± 3.60
13	<i>D. bellatulum</i>	> 100	> 100	9.66 ± 0.40	39.04 ± 3.65	84.00 ± 1.67	27.99 ± 1.28
14	<i>D. ochreatum</i>	> 100	> 100	1.89 ± 0.27	38.34 ± 2.44	45.25 ± 8.13	ND
15	<i>D. parishii</i>	> 100	> 100	4.09 ± 0.24	44.43 ± 3.58	40.74 ± 2.74	ND
16	<i>D. ellipsophyllum</i>	63.52 ± 0.69	> 100	6.53 ± 0.75	40.27 ± 5.75	55.71 ± 7.66	24.34 ± 2.95
17	<i>D. palpebrae</i>	> 100	> 100	4.77 ± 0.37	39.12 ± 3.04	41.92 ± 5.70	ND
18	<i>D. christyanum</i>	> 100	> 100	5.37 ± 0.08	34.13 ± 2.56	57.28 ± 4.21	5.21 ± 2.33
19	<i>D. cretaceum</i>	> 100	> 100	2.87 ± 0.24	39.71 ± 3.08	26.98 ± 3.34	ND
20	<i>D. fridericksianum</i>	> 100	> 100	2.10 ± 0.17	40.71 ± 2.39	40.06 ± 7.23	ND
21	<i>D. aphyllum</i>	> 100	> 100	2.36 ± 0.15	38.44 ± 4.68	23.78 ± 4.38	ND
22	<i>D. crumenatum</i>	> 100	> 100	3.57 ± 0.25	41.82 ± 1.73	31.80 ± 9.42	ND
23	<i>D. densiflorum</i>	> 100	> 100	1.63 ± 0.36	40.99 ± 4.80	14.64 ± 2.81	ND
24	<i>D. heterocarpum</i>	> 100	> 100	5.14 ± 0.42	38.12 ± 0.59	32.51 ± 6.67	ND
25	<i>D. kentrophyllum</i>	62.96 ± 0.46	26.58 ± 6.87	22.31 ± 0.34	37.10 ± 3.44	94.96 ± 1.40	24.67 ± 0.82
26	<i>D. harveyanum</i>	73.70 ± 0.18	85.74 ± 5.44	9.01 ± 1.03	37.71 ± 2.57	25.11 ± 3.41	27.88 ± 0.68
27	<i>D. cariniferum</i>	> 100	> 100	1.31 ± 0.02	40.97 ± 2.93	22.39 ± 2.71	ND
28	<i>D. gratiosissimum</i>	> 100	> 100	3.21 ± 0.48	41.91 ± 2.60	65.12 ± 3.02	ND
29	<i>D. fimbriatum</i>	> 100	> 100	2.00 ± 0.23	39.03 ± 1.23	14.02 ± 1.26	ND
	L-ascorbic acid	156.33 ± 1.68	7.43 ± 0.31*	44.95 ± 2.30*	—	—	—
	EGCG	—	—	—	59.71 ± 1.07*	91.98 ± 7.36	44.71 ± 7.17*

Notes: *p < 0.05 compared to test samples.

Abbreviation: ND, not detectable.

effects. Therefore, this plant was selected for further investigation of its phytochemical constituents. Phytochemical investigation of this plant resulted in the isolation of three flavonoids: kaempferol, quercetin, and rutin ([Supplementary Table S2](#)). The structures of the isolated compounds were determined by comparing their 1D- and 2D-NMR data with previously reported values.³¹

Cytotoxicity

The viability of BJ and HaCaT cells treated with various concentrations of *D. kentrophyllum* extract and its major compounds, kaempferol, quercetin, and rutin, is shown in [Figure 1](#). The results demonstrated that human fibroblast and keratinocyte viability rates did not differ from those of the control for all concentrations of the tested samples ($p>0.05$).

Inhibition of Intracellular ROS

UVB irradiation significantly enhanced ROS generation compared to non-irradiated cells ([Figure 2](#)). In fibroblasts, the concentration of *D. kentrophyllum* extract (6.25–100 $\mu\text{g/mL}$), kaempferol (12.5–100 μM), and quercetin (25–100 μM)

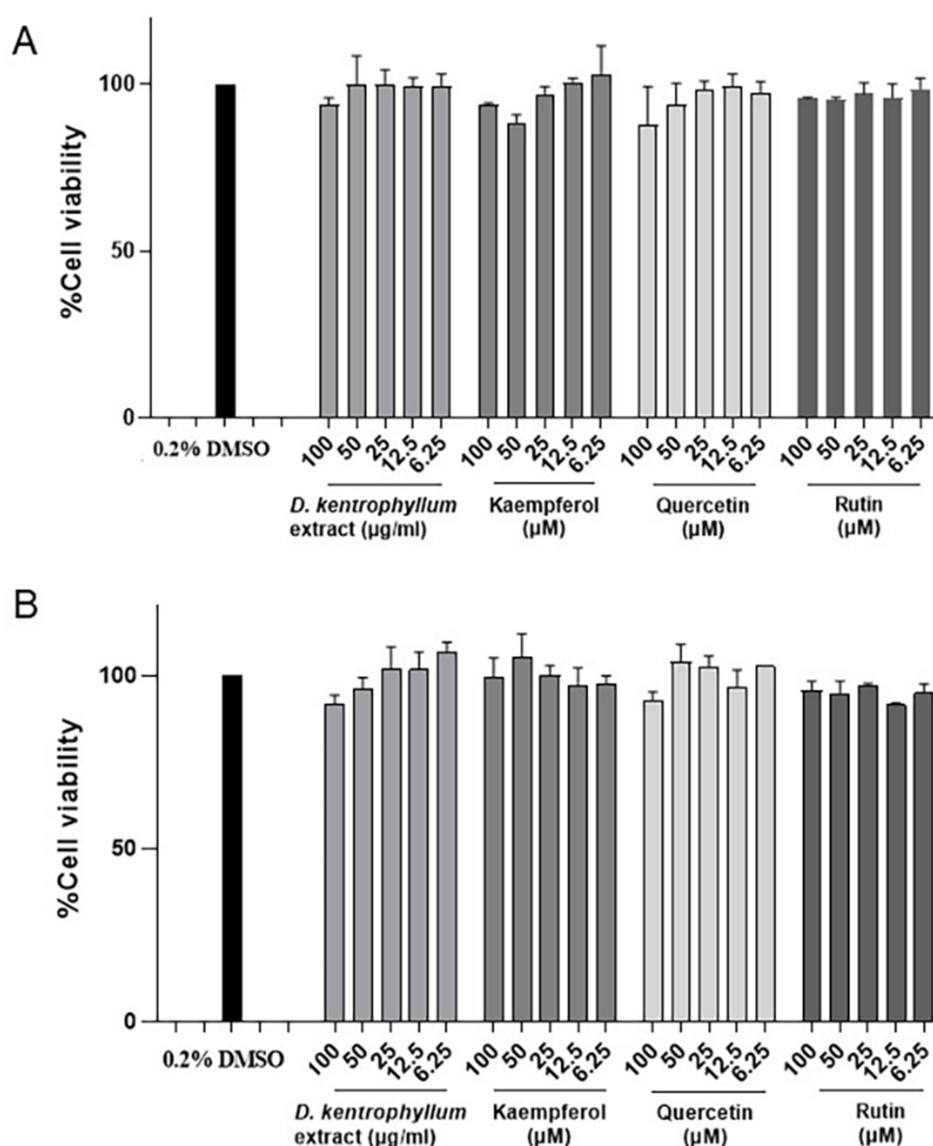


Figure 1 Human fibroblast (A) and human keratinocyte (B) viability cells after 24-h incubation with *D. kentrophyllum* extract, kaempferol, quercetin, and rutin. Data show the mean \pm SD (n=3).

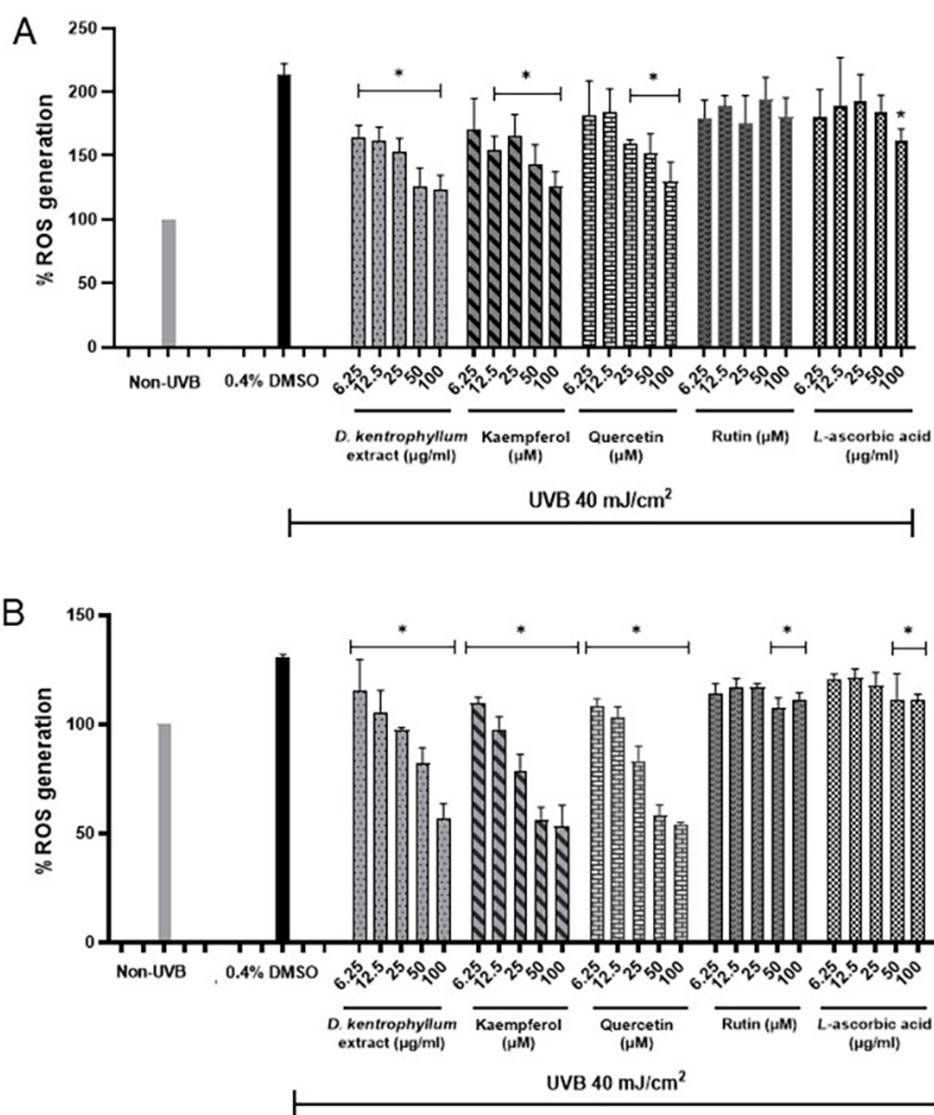


Figure 2 Effect of *D. kentrophyllum* extract, kaempferol, quercetin, rutin, and positive control (*L*-ascorbic acid) on the generation of ROS in UVB-irradiated human dermal fibroblasts (**A**) and keratinocytes (**B**). * $p < 0.05$ indicates a significant difference compared with UVB-irradiated cells.

significantly attenuated the ROS generation compared to UVB-irradiated cells ($213.23 \pm 9.27\%$) (Figure 2A). In contrast, *L*-ascorbic acid significantly suppressed ROS generation at 100 µg/mL. Pretreatment with *D. kentrophyllum* extract, kaempferol, and quercetin at all concentrations significantly diminished ROS generation in keratinocytes compared to UVB-irradiated cells ($130.56 \pm 1.52\%$) (Figure 2B). Rutin and *L*-ascorbic acid significantly decreased at concentration of 50–100 µM or µg/mL.

Construction of Phase Diagram

The regions representing the MEs are highlighted in black in Figure 3. They are transparent and have a low viscosity. No liquid crystalline structures were observed under cross-polarized light microscopy. In addition, a viscous gel-like consistency of MEs was observed in the gray areas (Figure 3). The ME region expanded as the ratio of Tween 80 to ethanol was increased from 1:1 to 5:1. The ratios 1:1, 3:1, and 5:1 were 11.11%, 18.13%, and 22.22%, respectively.

Based on these results, the Smix ratio was 5:1. The 0.4% of *D. kentrophyllum* extract was incorporated into a microemulsion formulation (DKME) containing 59.76% Smix (49.80% Tween 80 and 9.96% ethanol), isononyl isononanoate (9.96%), and water (29.88%) was prepared.

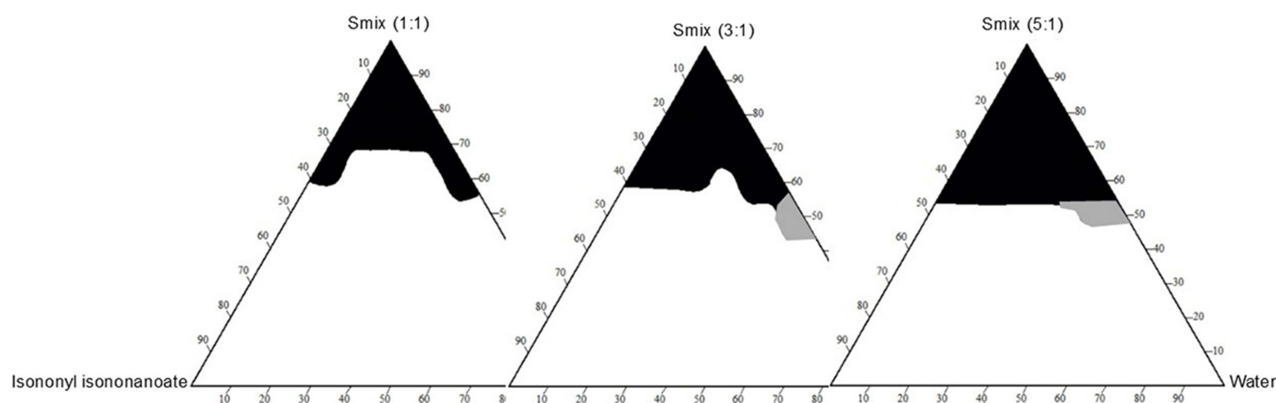


Figure 3 Pseudo ternary phase diagram for the Smix (Tween 80: ethanol), water, and isononyl isononanoate. Black and grey represent microemulsion regions under a polarized light microscope. The grey area indicates the high viscosity of MEs.

Characterization of ME Formulations

The DKME and MEB images are shown in [Figure 4](#). DKME is yellow-green and transparent. Birefringence of the formulations was not observed under a cross-polarized light microscope, indicating optical isotropy. In SAXS analysis, the 2D scattering pattern by the amplitude of the intensity modulation, which is observed in a cycle around the primary beam, represents the particle orientation. [Figure 5](#) shows that the scattering patterns of DKME and MEB are not aligned as liquid crystals, corresponding to the isotropic phase. The SAXS profile of the scattering intensity (I) and scattering vector (q) displayed a broad peak characteristic of the microemulsion system. The structure of the formulations was confirmed as microemulsions.³² The mean droplet size of both formulations was approximately 150 nm ([Table 2](#)). The PDI values of DKME and MEB are lower than 0.5, indicating droplet homogeneity.³³ From [Table 2](#), the zeta potential values were neutral due to the presence of non-ionic surfactant on the surface of microemulsion droplets, suggesting less stable and potential aggregation. The pH values of DKME and MEB ranged from 5.39 to 5.41, which were close to those of the human skin. The viscosity of DKME was $5,976 \pm 226.20$ cP, which was not significantly different from that of MEB ($p > 0.05$).

Stability Test of DKME

After eight cycles of heating and cooling, the optimized formulation was stable, with no change in appearance or optical properties, and no phase separation. The droplet size, PDI, zeta potential, pH, and viscosity were not significantly

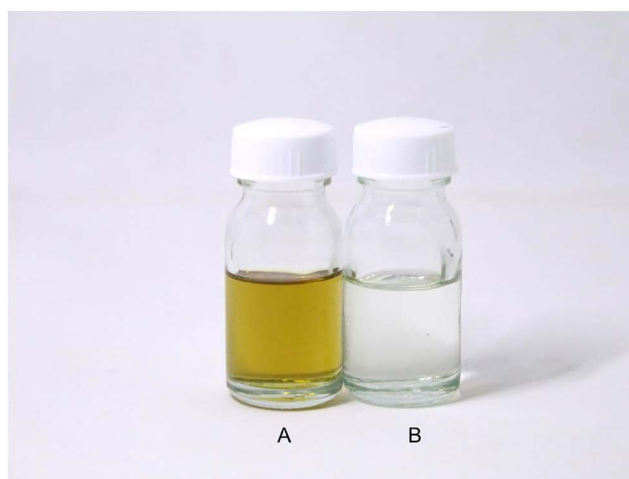


Figure 4 Appearance of the DKME (A) and MEB (B).

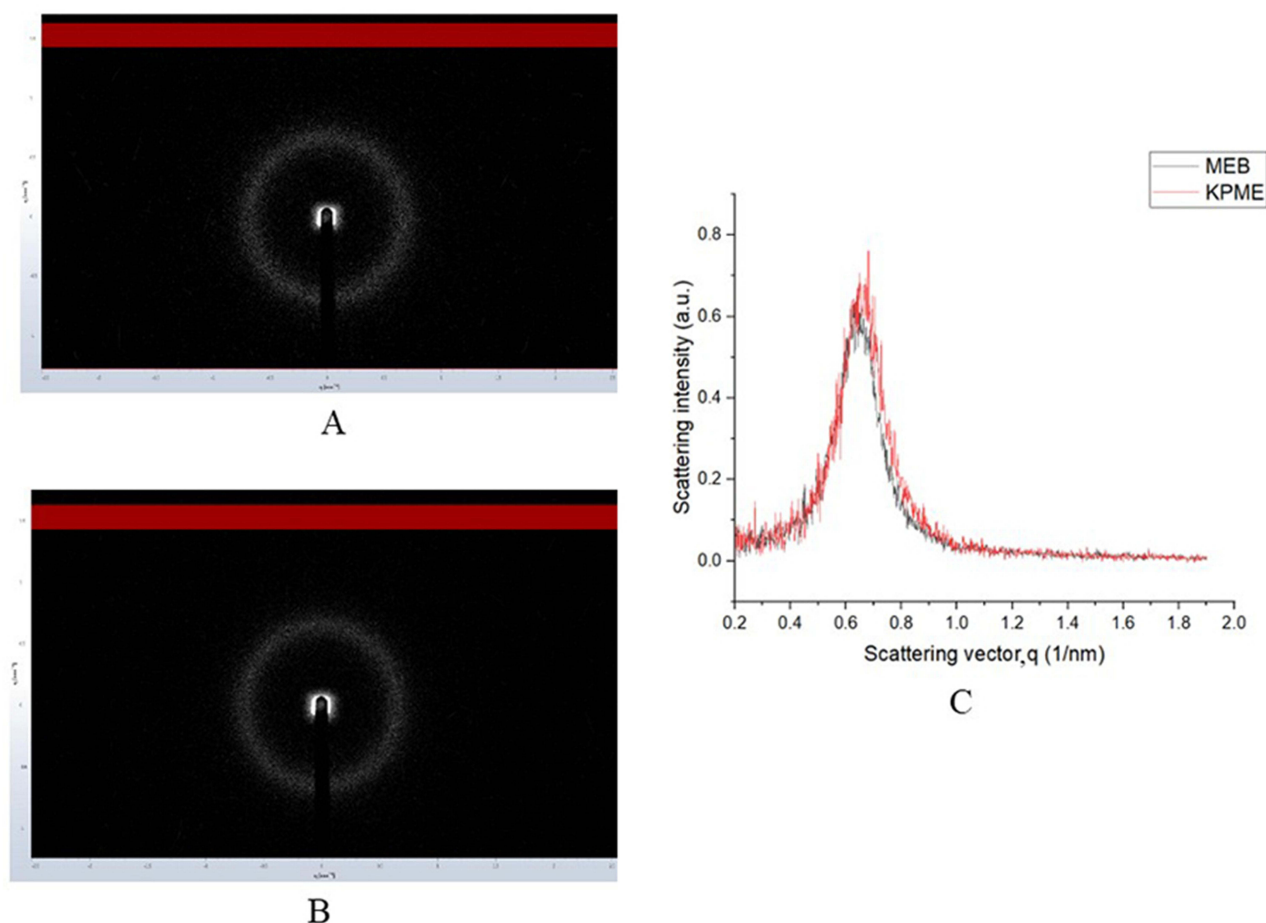


Figure 5 2D scattering patterns of the isotropic phase of DKME (A) and MEB (B) and their SAXS scattering pattern plotted by scattering intensity (I) vs scattering vector (q) (C).

different from the initial values ($p > 0.05$). Quercetin, an active compound in *D. kentrophyllum* extract, was not degraded during the stability study.

Cytotoxicity of DKME

The results of DKME toxicity in human fibroblasts and keratinocytes showed that DKME at a concentration of 6.25–200 $\mu\text{g/mL}$ was not significantly different from that of the untreated control (0.4% DMSO) in either cell line ($p > 0.05$) (Figure 6).

Discussion

ROS are major determinants of skin aging through the synthesis and expression of MMPs.² Finally, ECM, particularly collagen and elastin, is impaired, leading to wrinkle formation and elasticity loss. ROS are induced by UV radiation,

Table 2 Characteristics of the *D. Kentrophyllum* Extract-Loaded Microemulsion and Microemulsion Base ($n=3$)

Formulation	Droplet Size (nm)	Polydisperse index (PDI)	Zeta Potential (mV)	pH	Viscosity (mPa)
DKME	152.91 ± 5.35	0.45 ± 0.07	0.00 ± 0.07	5.39 ± 0.03	$5,976.00 \pm 159.27$
MEB	154.57 ± 2.82	0.44 ± 0.01	0.01 ± 0.08	5.41 ± 0.02	$6,012.11 \pm 243.76$

Abbreviations: DKME, *D. kentrophyllum* extract-loaded microemulsion; MEB, microemulsion base.

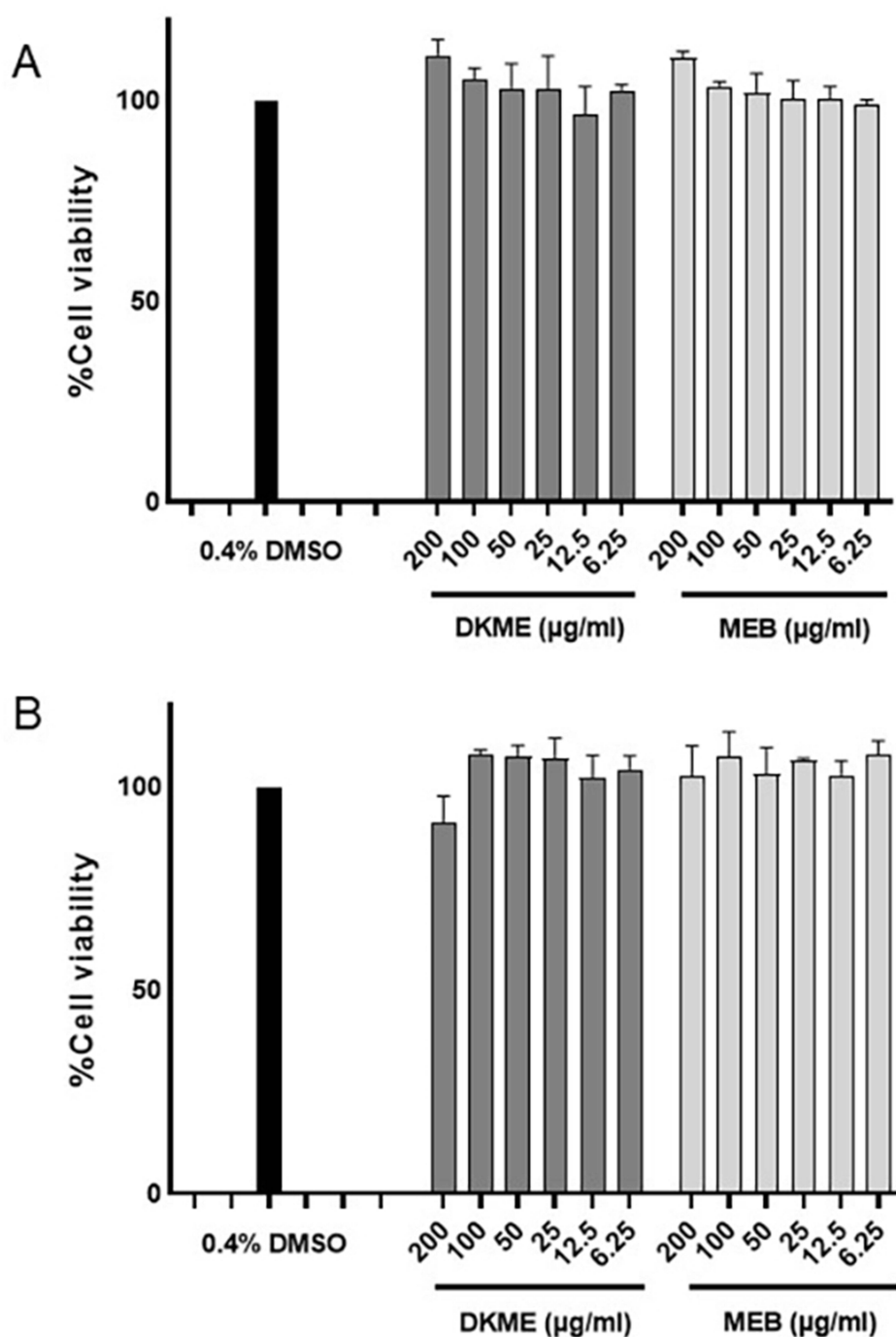


Figure 6 Human fibroblast (A) and human keratinocyte (B) viability cells after 24-h incubation with DKME and MEB. Data show the mean \pm SD (n=3).

including UVA and UVB. UVA damages epidermal keratinocytes and dermal fibroblasts in the long-term period, while UVB mainly affects the epidermis and upper part of the dermis. To reduce the ROS, natural compounds are widely used via antioxidant activities that can inhibit the formation of ROS or interrupt their propagation, causing regulated age-related signaling pathways, and delaying skin aging. In this study, the antioxidant capacities of 29 *Dendrobium* extracts were evaluated using three methods. They are based on electron transfer assays, namely, DPPH, H_2O_2 free radical scavenging, and FRAP assays. The DPPH assay is a simple and low-cost technique that is based on the electron donation of antioxidants to neutralize DPPH free radicals.³⁴ H_2O_2 can generate $\cdot OH$ - and ROS, eventually causing skin aging.³⁵

Electron donation of antioxidants may accordingly scavenge H_2O_2 into water and oxygen. The FRAP method measures the reduction of a complex of ferric ion (Fe^{3+})-ligand to ferrous complex (Fe^{2+}) by antioxidants under acid conditions.³⁶ Based on our results, *Dendrobium* extracts, especially *D. kentrophyllum*, are considered good electron donors. This can terminate the free radicals and delay the aging process. These capacities correlated with the TPC and TFC of the extracts (Supplementary Figures S3 and S4, and Table S1), which is supported by previous studies.^{17,18,34} TPC and TFC are important parameters for studying other extract properties. For example, in the study of Zulkifli et al (2020), the higher flavonoid content in defatted *Hylocereus polyrhizus* seed extract, obtained from suitable extraction system, was measured before isolating the major compounds.³⁷ Phuyal et al (2022) studied the TPC and TFC in different parts of *Zanthoxylum armatum* DC, followed by the study of antioxidant properties.³⁸ Therefore, high TPC and TFC in *D. kentrophyllum* extract are considered for further studies.

MMPs are zinc-containing endopeptidases that cleave collagen and other ECM proteins.³⁹ These enzymes can be stimulated by excessive intracellular ROS. MMP-1 and MMP-2 increase skin aging by activating fragmentation and degradation of collagen types I, II, III, and IV. Elastin interstitial fibers can be hydrolyzed by elastase, which further decreases skin elasticity. Phenolic compounds can inhibit MMPs by the interaction between their chemical functional groups, causing non-active enzymes.⁴⁰ *D. kentrophyllum* extract was expected to have good MMP-1, MMP-2, and elastase inhibition due to the richness of phenolic compounds. Three major phenolic compounds, quercetin, kaempferol, and rutin, were found in *D. kentrophyllum* extract, with 245 mg, 302 mg, and 84 mg, respectively (Supplementary Table S2). *D. kentrophyllum* extract is considered a good electron donor, with desirable antioxidant, anti-collagenase, and anti-elastase activities.

Natural compounds, such as resveratrol-enriched rice, red raspberry extract, polyphenolic-rich *Spatholobus suberectus* stem extract, citrus, and rosemary extracts have been studied for their anti-inflammatory and anti-enzymatic properties in the prevention of damage by UVB-induced ROS.^{41–44} To study the protective effect of *D. kentrophyllum* extract and its active compounds on intracellular ROS generation induced by UVB, BJ and HaCaT cells were exposed to UVB. A decrease in UVB-induced intracellular ROS might result in the presence of its active constituents in *D. kentrophyllum* extract. These results are consistent with those of previous studies, demonstrating that quercetin and rutin can inhibit ROS in keratinocytes and fibroblasts.^{45,46} A key safety profile of natural extracts and substances is biocompatibility testing involving cell viability and cytotoxicity.⁴⁷ Cell viability refers to the proportion of healthy, functioning cells in a sample, whereas cytotoxicity assesses the ability of a substance to induce cell damage or death. According to our study, *D. kentrophyllum* extract and its active compounds were non-toxic to human skin.⁴⁸ Based on combined observations, *D. kentrophyllum* is a potential anti-aging agent and can be reasonably used in product development.

Recently, MEs have been of interest in the pharmaceutical and cosmeceutical aspects owing to their features. MEs are thermodynamically stable, solubilize both hydrophilic and hydrophobic substances, and improve skin permeation.^{49–51} MEs can be easily prepared by mixing a suitable ratio of surfactants, oil, and water phases. Major concerns in the development of microemulsions are their acceptability and safety. Non-ionic surfactants that exhibit the lowest irritation are widely used to reduce the surface area between the oil and water molecules.⁵² Tween 80 is a well-known safe non-ionic surfactant. It is frequently used in various pharmaceutical formulations since it improves drug solubility and enhances permeation and bioavailability.⁵³ Furthermore, short-chain alcohol such as ethanol is mostly used in microemulsions since it affects the particle size and causes a reduction of the rigid structures.⁵⁴ In this study, Tween 80 and ethanol were therefore used as surfactant and cosurfactant, respectively. Isononyl isononanoate, non-greasy emollient, was used as oil.

As a result of the MEs obtained in the pseudo-ternary phase diagram, ethanol considerably affected the ME formation. One possible reason for this is that ethanol was incorporated into the interface, resulting in a reduction in the relative concentration of Tween 80. The density of the surfactant at the oil–water interface subsequently decreases, causing insufficient capability to maintain the interfacial tension between oil and water. This leads to a decrease in the microemulsion region.⁵⁵

The suitable dose of the extract affects the effectiveness of the formulation. From Isnaini study, 5–10 times of EC_{50} according to DPPH free radical of the tamarind fruit pulp extract was used to determine the concentration in the lotion formulation, which displayed the existence of antioxidant activity.⁵⁶ Based on the result of the inhibition of intracellular ROS, therefore, 0.4% *D. kentrophyllum* extract was incorporated.

Droplet size is a dominant parameter that influences the physical behavior and functionality of topical formulations, that is stability and drug penetration. Hashem et al revealed that clotrimazole-loaded microemulsions with a size of 200

nm significantly penetrated and remained within the skin compared to conventional creams.⁵⁷ Therefore, measurable sizes could be facilitated in the skin. The skin permeation of DKME should be studied further to determine its effectiveness. PDI represents the particle size distribution. In this study, the PDI values of MEB and DKME were lower than 0.5, indicating particle homogeneity.³³ Zeta potential generally indicates the surface charge of the particles, and refers to the amount of repulsive force between the formed droplets, indicating the physical stability of the preparations. The high zeta potential value of (\pm)30 mV is responsible for its good stability. Conversely, zeta potential values between -10 and 10 mV represent a neutral surface.⁵⁸

To date, DKME has been stable in preliminary stability tests. However, long-term stability is required for further studies.

To predict the negative result of in vivo effects, the in vitro cytotoxicity of the developed formulation is suggested.⁵⁹ In this study, the toxicity of DKME to human fibroblast and keratinocyte cells was studied, and no cytotoxicity was observed. Therefore, DKME is a promising topical cosmeceutical for anti-aging applications.

Conclusion

Dendrobium extracts have the potential to be used as anti-aging bioactive ingredients because of their antioxidant, anti-collagenase, and anti-elastase activities. Based on the most potent anti-aging activities, *D. kentrophyllum* extract was further investigated. *D. kentrophyllum* extract is safe for human skin cells and can decrease the intracellular ROS levels induced by UVB. The microemulsion formulation of *D. kentrophyllum* comprising 49.80% Tween 80, 9.96% ethanol, 9.96% isononyl isononanoate, 29.88% water, and 0.40% *D. kentrophyllum* extract exhibited desirable characteristics with good physical and chemical stability. This formulation is non-toxic and, consequently, may be proposed as an anti-aging topical product. The novelty of this work is the investigation of anti-aging effect of *Dendrobium* spp. as well as novel microemulsions containing the potential usage of *Dendrobium*. The study on using *Dendrobium* spp. in cosmeceutical products is still limited. This work is, therefore, considered the first investigation to increase the value of medicinal plants in the cosmeceutical aspect. In summary, *D. kentrophyllum* can be considered as a promising natural compound for producing anti-aging products using microemulsions and may be applied to other nanocarrier systems. However, in vivo studies on skin irritation and efficacy of this product might be conducted in further study.

Acknowledgments

The authors are grateful to the Faculty of Pharmaceutical Sciences, Chulalongkorn University, and the Faculty of Integrative Medicine, Rajamangala University of Technology Thanyaburi, for supporting this work.

Author Contributions

NN and BS contributed to the conceptualization of the study. BS performed herbal extraction and purification. ST performed antioxidant testing and formulation development. NW performed the cell works and interpreted the data. NK tested enzymatic activity. ST wrote the first draft of the manuscript. NN revised the manuscript. All authors contributed to manuscript revision and approved the submitted version.

All authors made a significant contribution to the work reported, whether that is in the conception, study design, execution, acquisition of data, analysis and interpretation, or in all these areas; took part in drafting, revising or critically reviewing the article; gave final approval of the version to be published; have agreed on the journal to which the article has been submitted; and agree to be accountable for all aspects of the work.

Disclosure

The authors report no conflicts of interest in this work.

References

1. Chen J, Liu Y, Zhao Z, et al. Oxidative stress in the skin: impact and related protection. *Int J Cosmet Sci*. 2021;43(5):495–509. doi:10.1111/ics.12728
2. Freitas-Rodriguez S, Folgueras AR, Lopez-Otin C. The role of matrix metalloproteinases in aging: tissue remodeling and beyond. *Biochim Biophys Acta mol Cell Res*. 2017;1864(11 Pt A):2015–2025. doi:10.1016/j.bbamcr.2017.05.007

3. Pittayapruk P, Meephansan J, Prapapan O, et al. Role of matrix metalloproteinases in photoaging and photocarcinogenesis. *Int J mol Sci.* **2016**;17(6):868. doi:10.3390/ijms17060868
4. Chatatikun M, Chiabchalard A. Thai plants with high antioxidant levels, free radical scavenging activity, anti-tyrosinase and anti-collagenase activity. *BMC Complement Altern Med.* **2017**;17(1):487. doi:10.1186/s12906-017-1994-7
5. Rungruang R, Ratanathavorn W, Boohuad N, et al. Antioxidant and anti-aging enzyme activities of bioactive compounds isolated from selected Zingiberaceae plants. *Agric Nat Resour.* **2021**;55:153–160. doi:10.34044/j.anres.2021.55.1.20
6. Pientaweeratch S, Panapisal V, Tansirikongkol A. Antioxidant, anti-collagenase and anti-elastase activities of *Phyllanthus emblica*, *Manilkara zapota* and silymarin: an *in vitro* comparative study for anti-aging applications. *Pharm Biol.* **2016**;54(9):1865–1872. doi:10.3109/13880209.2015.1133658
7. Thring TS, Hili P, Naughton DP. Anti-collagenase, anti-elastase and anti-oxidant activities of extracts from 21 plants. *BMC Complement Altern Med.* **2009**;9:27. doi:10.1186/1472-6882-9-27
8. Wang YH. Traditional uses and pharmacologically active constituents of *Dendrobium* plants for dermatological disorders: a review. *Nat Prod Bioprospect.* **2021**;11(5):465–487. doi:10.1007/s13659-021-00305-0
9. Peyachoknagul S, Mongkolsirawatana C, Srikulnath S, et al. Identification of native *Dendrobium* species in Thailand by PCR-RFLP of rDNA-ITS and chloroplast DNA. *Sci Asia.* **2014**;40:113–120. doi:10.2306/scienceasia1513-1874.2014.40.113
10. Pengdee C, Sritularak B, Putalun W. Optimization of microwave-assisted extraction of phenolic compounds in *Dendrobium formosum* Roxb. ex Lindl. and glucose uptake activity. *S Afr J Bot.* **2020**;132:423–431. doi:10.1016/j.sajb.2020.06.009
11. Mou Z, Zhao Y, Ye F, et al. Identification, biological activities and biosynthetic pathway of *Dendrobium* alkaloids. *Front Pharmacol.* **2021**;12:605994. doi:10.3389/fphar.2021.605994
12. Lam Y, Ng TB, Yao RM, et al. Evaluation of chemical constituents and important mechanism of pharmacological biology in dendrobium plants. *Evid Based Complement Alternat Med.* **2015**;2015:841752. doi:10.1155/2015/841752
13. Guo L, Qi J, Du D, et al. Current advances of *Dendrobium officinale* polysaccharides in dermatology: a literature review. *Pharm Biol.* **2020**;58(1):664–673. doi:10.1080/13880209.2020.1787470
14. Kanlayavattanakul M, Lourith N, Chaikul P. *Dendrobium* orchid polysaccharide extract: preparation, characterization and *in vivo* skin hydrating efficacy. *Chin Herb Med.* **2019**;11(4):400–405. doi:10.1016/j.chmed.2019.03.012
15. Li Y, Cao Z, Li Q, et al. Effects of *Dendrobium* polysaccharides on the functions of human skin fibroblasts and expression of matrix metalloproteinase-2 under high-glucose conditions. *Int J Endocrinol.* **2021**;2021:1092975. doi:10.1155/2021/1092975
16. Kanlayavattanakul M, Pawakongbun T, Lourith M. Biological activity and phytochemical profiles of *Dendrobium*: a new source for specialty cosmetic materials. *Ind Crops Prod.* **2018**;120:61–70. doi:10.1016/j.indcrop.2018.04.059
17. Kongkatitham V, Muangnoi C, Kyokong N, et al. Anti-oxidant and anti-inflammatory effects of new bibenzyl derivatives from *Dendrobium parishii* in hydrogen peroxide and lipopolysaccharide treated RAW264.7 cells. *Phytochem Lett.* **2018**;24:31–38. doi:10.1016/j.phytol.2018.01.006
18. Ma RJ, Yang L, Bai X, et al. Phenolic constituents with antioxidative, tyrosinase inhibitory and anti-aging activities from *Dendrobium loddigesii* Rolfe. *Nat Prod Bioprospect.* **2019**;9(5):329–336. doi:10.1007/s13659-019-00219-y
19. Schuster D. *Encyclopedia of Emulsion Technology: Volume 4*. Boca Raton: CRC Press; **1996**.
20. Suhail N, Alzahrani A, Basha WJ, et al. Microemulsions: unique properties, pharmacological applications, and targeted drug delivery. *Front Nanotechnol.* **2021**;3:754889. doi:10.3389/fnano.2021.754889
21. Prommaban A, Chaityana W. Microemulsion of essential oils from citrus peels and leaves with anti-aging, whitening, and irritation reducing capacity. *J Drug Deliv Sci Technol.* **2022**;69:103188. doi:10.1016/j.jddst.2022.103188
22. Marsup P, Sirilun S, Prommaban A, et al. Potential of topical microemulsion serum formulations to enhance *in vitro* and clinical anti-skin wrinkle benefits of *Cordyceps militaris* extracts. *Res Sq.* **2021**. doi:10.21203/rs.3.rs-550591/v1
23. Warinhomhoun S, Muangnoi C, Buranasudja V, et al. Antioxidant activities and protective effects of dendropachol, a new bisbibenzyl compound from *Dendrobium pachyglossum*, on hydrogen peroxide-induced oxidative stress in HaCaT keratinocytes. *Antioxidants.* **2021**;10(2):252. doi:10.3390/antiox10020252
24. Al-Amiery AA, Al-Majedy YK, Kadhum AA, et al. Hydrogen peroxide scavenging activity of novel coumarins synthesized using different approaches. *PLoS One.* **2015**;10(7):e0132175. doi:10.1371/journal.pone.0132175
25. Zhang W, Wang Z, Ganesan K, et al. Antioxidant activities of aqueous extracts and protein hydrolysates from marine worm hechong (*Tylorhynchus heterochaeta*). *Foods.* **2022**;11(13):1837. doi:10.3390/foods11131837
26. Luo J, Cai W, Wu T, et al. Phytochemical distribution in hull and cotyledon of adzuki bean (*Vigna angularis* L.) and mung bean (*Vigna radiata* L.), and their contribution to antioxidant, anti-inflammatory and anti-diabetic activities. *Food Chem.* **2016**;201:350–360. doi:10.1016/j.foodchem.2016.01.101
27. Boran R. Investigations of anti-aging potential of *Hypericum origanifolium* Willd. for skincare formulations. *Ind Crops Prod.* **2018**;118:290–295. doi:10.1016/j.indcrop.2018.03.058
28. Zhu ML, Zhang PM, Jiang M, et al. Myricetin induces apoptosis and autophagy by inhibiting PI3K/Akt/mTOR signalling in human colon cancer cells. *BMC Complement Med Ther.* **2020**;20(1):209. doi:10.1186/s12906-020-02965-w
29. Xiao Z, Yang S, Chen J, et al. Trehalose against UVB-induced skin photoaging by suppressing MMP expression and enhancing procollagen I synthesis in HaCaT cells. *J Funct Foods.* **2020**;74:104198. doi:10.1016/j.jff.2020.104198
30. Thiangtham J. Determination of Antioxidant Constituents in the Medicinal Plant *Cissus quadrangularis* Linn [dissertation]. Bangkok: Chulalongkorn University; **2003**.
31. Lin LJ, Huang XB, Lv ZC. Isolation and identification of flavonoids components from *Pteris vittata* L. *Springerplus.* **2016**;5(1):1649. doi:10.1186/s40064-016-3308-9
32. Carvalho AL, Silva JA, Lira AA, et al. Evaluation of microemulsion and lamellar liquid crystalline systems for transdermal zidovudine delivery. *J Pharm Sci.* **2016**;105(7):2188–2193. doi:10.1016/j.xphs.2016.04.013
33. Dehghani F, Farhadian N, Golmohammadzadeh S, et al. Preparation, characterization and *in-vivo* evaluation of microemulsions containing tamoxifen citrate anti-cancer drug. *Eur J Pharm Sci.* **2017**;96:479–489. doi:10.1016/j.ejps.2016.09.033
34. Moyo B, Oyedemi S, Masika PJ, et al. Polyphenolic content and antioxidant properties of *Moringa oleifera* leaf extracts and enzymatic activity of liver from goats supplemented with *Moringa oleifera* leaves/sunflower seed cake. *Meat Sci.* **2012**;91(4):441–447. doi:10.1016/j.meatsci.2012.02.029
35. Masaki H. Role of antioxidants in the skin: anti-aging effects. *J Dermatol Sci.* **2010**;58(2):85–90. doi:10.1016/j.jdermsci.2010.03.003

36. Munteanu IG, Apetrei C. Analytical methods used in determining antioxidant activity: a review. *Int J mol Sci.* **2021**;22(7):3380. doi:10.3390/ijms22073380
37. Zulkifli SA, Abd Gani SS, Zaidan UH, et al. Optimization of total phenolic and flavonoid contents of defatted pitaya (*Hylocereus polyrhizus*) seed extract and its antioxidant properties. *Molecules.* **2020**;25(4):787. doi:10.3390/molecules25040787
38. Phuyal N, Jha PK, Raturi PP, et al. Total Phenolic, Flavonoid Contents, and Antioxidant Activities of Fruit, Seed, and Bark Extracts of *Zanthoxylum armatum* DC. *ScientificWorldJournal.* **2020**;2020:8780704. doi:10.1155/2020/8780704
39. Shin JW, Kwon SH, Choi JY, et al. Molecular mechanisms of dermal aging and antiaging approaches. *Int J mol Sci.* **2019**;20(9):2126. doi:10.3390/ijms20092126
40. Madhan B, Krishnamoorthy G, Rao JR, et al. Role of green tea polyphenols in the inhibition of collagenolytic activity by collagenase. *Int J Biol Macromol.* **2007**;41(1):16–22. doi:10.1016/j.ijbiomac.2006.11.013
41. Subedi L, Lee TH, Wahedi HM, et al. Resveratrol-enriched rice attenuates UVB-ROS-induced skin aging via downregulation of inflammatory cascades. *Oxid Med Cell Longev.* **2017**;2017:8379539. doi:10.1155/2017/8379539
42. Wang PW, Cheng YC, Hung YC, et al. Red raspberry extract protects the skin against UVB-induced damage with antioxidative and anti-inflammatory properties. *Oxid Med Cell Longev.* **2019**;2019:9529676. doi:10.1155/2019/9529676
43. Kwon KR, Alam MB, Park JH, et al. Attenuation of UVB-induced photo-aging by polyphenolic-rich *Spatholobus suberectus* stem extract via modulation of MAPK/AP-1/MMPs signaling in human keratinocytes. *Nutrients.* **2019**;11(6):1341. doi:10.3390/nu11061341
44. Perez-Sanchez A, Barrajon-Catalan E, Caturla N, et al. Protective effects of citrus and rosemary extracts on UV-induced damage in skin cell model and human volunteers. *J Photochem Photobiol B.* **2014**;136:12–18. doi:10.1016/j.jphotobiol.2014.04.007
45. Zhu X, Li N, Wang Y, et al. Protective effects of quercetin on UVB irradiation-induced cytotoxicity through ROS clearance in keratinocyte cells. *Oncol Rep.* **2017**;37(1):209–218. doi:10.3892/or.2016.5217
46. Choi SJ, Lee SN, Kim K, et al. Biological effects of rutin on skin aging. *Int J Mol Med.* **2016**;38(1):357–363. doi:10.3892/ijmm.2016.2604
47. Sukumaran A, Sweetey VK, Vikas B, et al. Cytotoxicity and cell viability assessment of biomaterials. In: Sukumaran A, Mansour MA, editors. *Cytotoxicity - Understanding Cellular Damage and Response.* IntechOpen; **2023**.
48. Nemudzhivadi V, Masoko P. *In vitro* assessment of cytotoxicity, antioxidant, and anti-inflammatory activities of *Ricinus communis* (Euphorbiaceae) leaf extracts. *Evid Based Complement Alternat Med.* **2014**;2014:625961. doi:10.1155/2014/625961
49. Leanpolchareanchai J, Padois K, Falson F, et al. Microemulsion system for topical delivery of Thai Mango seed kernel extract: development, physicochemical characterisation and *ex vivo* skin permeation studies. *Molecules.* **2014**;19(11):17107–17129. doi:10.3390/molecules191117107
50. Assaf SM, Maarouf KT, Altaani BM, et al. Jojoba oil-based microemulsion for transdermal drug delivery. *Res Pharm Sci.* **2021**;16(4):326–340. doi:10.4103/1735-5362.319572
51. Kuropakornpong P, Itharat A, Ooraikul B, et al. Development and optimization of Benjakul microemulsion formulations for enhancing topical anti-inflammatory effect and delivery. *Res Pharm Sci.* **2022**;17(2):111–122. doi:10.4103/1735-5362.335170
52. Effendy I, Maibach HI. Surfactants and experimental irritant contact dermatitis. *Contact Dermatitis.* **1995**;33(4):217–225. doi:10.1111/j.1600-0536.1995.tb00470.x
53. Kaur G, Mehta SK. Developments of polysorbate (Tween) based microemulsions: preclinical drug delivery, toxicity and antimicrobial applications. *Int J Pharm.* **2017**;529(1–2):134–160. doi:10.1016/j.ijpharm.2017.06.059
54. Szumala P. Structure of microemulsion formulated with monoacylglycerols in the presence of polyols and ethanol. *J Surfactants Deterg.* **2015**;18(1):97–106. doi:10.1007/s11743-014-1618-x
55. Song X, Wang J, Li S, et al. Formation of Sacha inchi oil microemulsion systems: effects of non-ionic surfactants, short-chain alcohols, straight-chain esters and essential oils. *J Sci Food Agric.* **2022**;102(9):3572–3580. doi:10.1002/jsfa.11703
56. Isnaini N, Songkro S, Kaewnopparat N, et al. Formulation and investigation of antioxidant potential of O/W lotions containing *Tamarindus indica* L. fruit pulp extract. *Matter.* **2019**;5(2):100–112. doi:10.20319/mijst.2019.52.100112
57. Hashem FM, Shaker DS, Ghorab MK, et al. Formulation, characterization, and clinical evaluation of microemulsion containing clotrimazole for topical delivery. *AAPS Pharm Sci Tech.* **2011**;12(3):879–886. doi:10.1208/s12249-011-9653-7
58. Patravale V, Dandekar P, Jain R. Characterization techniques for nanoparticulate carriers. In: Patravale V, Dandekar P, Jain R, editors. *Nanoparticulate Drug Delivery.* Cambridge: Woodhead Publishing; **2012**:87–121.
59. Ildikó B, Dániel N, Ferenc F, et al. Role of cytotoxicity experiments in pharmaceutical development. In: Tülay Aşkin Ç, editor. *Cytotoxicity.* IntechOpen; **2017**.